Semiflexible polymer in the cactus approximation

M. Pretti
Istituto Nazionale per la Fisica della Materia (INFM) and Dipartimento di Fisica, Politecnico di Torino, Corso Duca degli Abruzzi 24, I-10129 Torino, Italy

(Received 1 October 2002; published 30 December 2002)

We investigate a cactus approximation for the analysis of a lattice polymer model (self-avoiding walk) in two and three dimensions. We focus on the semiflexible model, which incorporates both an attractive short range interaction between monomers that are nonconsecutive along the chain, and a bending energy (stiffness). In agreement with Monte Carlo simulations, we find two different qualitative behaviors. In the low stiffness regime the polymer undergoes two different transitions upon decreasing temperature: an ordinary Θ collapse from a swollen (''coil'') state to a disordered compact (''globule'') state, and then a first-order transition to an orientationally ordered (''anisotropic'') state. In the high stiffness regime the system displays a single first-order collapse from the coil state at high temperature to the anisotropic state at low temperature. We show that the cactus approximation is able to recover even fine qualitative features of the phase diagram, such as the stiffness dependence of the Θ temperature, with a relatively small computational effort.

DOI: 10.1103/PhysRevE.66.061802 PACS number(s): 61.25.Hq, 05.50.+q, 05.70.Fh, 64.60.Cn

I. INTRODUCTION

Lattice Self-Avoiding Walk (SAW) models, i.e., random walks that are forbidden to visit lattice sites more than once, are usually employed to describe linear polymers in a good solvent [1,2]. Each site visited by the walk represents a monomer (or a cluster of monomers), and the segments (steps) of the walk define a configuration of the polymer chain [3]. A short range interaction between monomers that are nonconsecutive along the chain is also generally considered in order to model either Van der Waals attractive forces between monomers or the effective result of hydrophobic repulsion between monomers and solvent (water) molecules. Such interactions cause the well-known Θ transition from a swollen coil at high temperature to a compact globule at low temperature [4,5].

In order to describe more complex physics, concerning for instance biological macromolecules, further details usually need to be included in the model. Motivated by such interests, Bascle, Garel, and Orland [6] have tried to describe the formation of protein α helices [7] in the framework of Hamiltonian walk models (SAWs forced to visit all lattice sites). They have proposed a model which assigns an energy cost to the formation of a corner in the walk (bending energy). The latter should represent hydrogen-bond breaking in a single helical turn, giving rise to a competition between entropy gain and energy cost of breaking hydrogen-bonded ordered structures. For such a model the mean-field theory [6] predicts, upon increasing temperature, a first-order transition between a quasifrozen anisotropic phase, in which the fraction of corners is very close to zero, to a molten phase with a significant fraction of corners. The model has been extended to the ordinary SAW (not a Hamiltonian walk), adding the usual monomer-monomer attractive energy, in order to investigate the nature of the collapse [8]. This is known as the semiflexible polymer model, which has been studied both in the mean-field approach [8] and by means of accurate Monte Carlo simulations [9,10]. It turns out that a single semiflexible chain in solution may have different behaviors, depending on stiffness, that is, on the energy cost assigned to corner formation. In the low stiffness regime, upon decreasing temperature, the polymer undergoes a Θ collapse from a swollen (''coil'') state to a disordered compact (''globule'') state, and then a first-order transition to a quasifrozen ordered (''anisotropic'') state. The last one is very similar to the ordered state observed in the Hamiltonian walk model. It is anisotropic and dense: most polymer segments are aligned and the SAW is forced to visit (almost) all lattice sites (quasi-Hamiltonian walk). In the high stiffness regime a direct first-order collapse from the coil to the anisotropic state takes place.

Apart from the relevance of the semiflexible model to describing real polymer physics (such as ordered structure formation in biopolymers), in this paper, we are interested in the performance of the cactus approximation, compared to different methods that have been previously employed to investigate this relatively simple model, whose phase diagram is presently known with some accuracy. The cactus approximation for a given polymer model consists in approximating the behavior of a single SAW on an ordinary lattice by that of a gas of SAWs with the same interactions on a suitable cactus tree (Husimi tree). The analysis of the latter system can be performed exactly [11,12]. We choose a Husimi tree made up of squares, to approximate the two-dimensional (2D) square lattice, and one made up of cubes, to approximate the 3D simple cubic lattice, with a connectivity constant equal to 2 in both cases. We work out the grand-canonical phase diagram (chemical potential vs temperature) for two different cases, in the low and high stiffness regimes, respectively. Moreover, we investigate the dilute solution (single chain) limit, reporting the polymer density and configurational entropy as a function of temperature. Finally, the dilute solution limit is characterized in full detail by determining the stiffness vs temperature and stiffness vs entropy phase diagrams. The former is compared to Monte Carlo simulations for the 3D case [9,10], showing that the cactus approximation recovers a qualitatively correct phase behavior. Moreover, we compare our results with previously performed mean-field-like investigations: the ordinary mean-field theory [8] and the Bethe approximation [13,14]. The

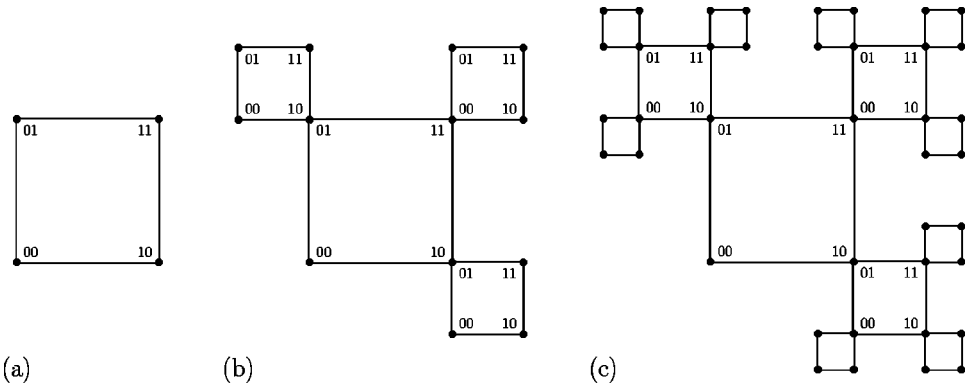

FIG. 1. Growth procedure to build the square cactus: (a) first-generation branch; (b) second-generation branch; (c) third-generation branch. Binary numerals denote different sites in each square, according to the convention explained in the text.

Bethe approximation is a classical tool of statistical mechanics, which improves the ordinary mean-field theory, treating exactly nearest neighbor correlations [15]. It has been reformulated under different points of view [16–18], but is actually equivalent, apart from details, to the cactus approximation for a Cayley tree [19], a special case of Husimi tree made up of nearest neighbor pairs. As far as the semiflexible model is concerned, the ordinary mean-field approach does not describe satisfactorily the high stiffness regime, and does not predict the direct coil-anisotropic transition. The Bethe approximation yields a qualitatively correct phase diagram with two different regimes [13], but introduces some artifacts. For example, the Θ collapse is absolutely unaffected by stiffness. On the contrary, the cactus approximation correctly recovers also the stiffness dependence of the Θ temperature, which turns out to increase upon increasing stiffness, in agreement with Monte Carlo simulations.

The paper is organized as follows. In Sec. II, we describe the semiflexible model in some more detail, and introduce the cactus approximation, which in principle should work for a generic interacting SAW model on a d-dimensional hypercubic lattice. In Sec. III, we present the results, showing the grand-canonical (chemical potential vs temperature) phase diagram, both in the low and high stiffness regimes, and the dilute solution phase diagrams. 3D results are compared both to 2D ones and to previous investigations on the semiflexible model. Section IV is devoted to a summary of the results and to some concluding remarks.

II. THE MODEL AND THE CACTUS APPROXIMATION

Let us consider a SAW on a hypercubic lattice in d dimensions. Each site visited by the walk represents a monomer. Empty sites represent clusters of solvent molecules. An attractive energy $-\varepsilon$ (with $\varepsilon>0$) is assigned to each pair of nonconsecutive monomers placed on nearest neighbor sites. According to the grand-canonical description, a chemical potential μ is associated to each monomer, while the solvent chemical potential is conventionally assumed to be zero. An energy cost χ (with $\chi>0$) is taken into account for each visited site in which the polymer bends. The χ parameter is a way of describing polymer stiffness, therefore, it will be referred to as stiffness parameter in the following.

Let us now introduce the cactus approximation. Basically it consists in replacing the single SAW on the ordinary lattice by a gas of mutually avoiding and self-avoiding walks with the same interactions on a suitable Husimi tree (cactus tree). Dealing with a hypercubic lattice in d dimensions, we choose a cactus made up of d-dimensional hypercubes (d cubes), with a connectivity constant equal to 2 (each site shared by 2 d cubes). The cactus tree may be obtained as the result of a recursive growth procedure. Figure 1 shows the growth of a branch of our cactus tree for the $d=2$ case, which is usually referred to as square cactus. With a connectivity constant equal to 2, the complete cactus is made up of two such branches. A three- or higher-dimensional cactus can be obtained by a similar procedure.

The state of the system can be defined by specifying, for each lattice site, (i) whether the site is empty or visited by a walk and, in the latter case, (ii) the chain configuration on that site, that is, the directions of two segments (towards the previous and next monomer along the chain). It is then useful to introduce for each site a suitable state variable σ. The correspondence between values of σ and local (site) configurations can be chosen arbitrarily. In Table I, we report our ''encoding'' for $d=2$. Let us notice that $\sigma=0$ corresponds to an empty site and $\sigma>0$ to an occupied site. Moreover, $\sigma \leqslant 2$ denotes a ''straight'' segment, while $\sigma>2$ denotes a ''bent'' segment. The encoding can be easily extended to $d=3$, so we do not report it explicitly for the latter case. Let us notice that, in order to preserve polymer connectivity, site state variables have to satisfy certain constraints. Namely, if two given sites are nearest neighbors, and the configurational state of the former is such that it is linked (not linked) to the latter by a chain segment, then also the latter site must be in

TABLE I. Correspondence between local configurations and values of the site state variable in $d=2$.

σ	0	1	2	3	4	5	6

TABLE II. Pair interaction energies $u_x(\sigma,\sigma')$ (a) and $u_y(\sigma,\sigma')$ (b) in $d=2$. Notice that σ' follows σ along each axis; $u_x(\sigma,\sigma')=\infty$ $[u_y(\sigma,\sigma')=\infty]$ corresponds to pair states σ,σ' that violate the connectivity constraint along the x (y) axis.

σ'	0		1		2		3		4		5		6	
σ	(a)	(b)	(a)	(b)	(a)	(b)	(a)	(b)	(a)	(b)	(a)	(b)	(a)	(b)
0	0	0	∞	0	0	∞	0	0	∞	0	∞	∞	0	∞
1	∞	0	0	$-\varepsilon$	∞	∞	∞	$-\varepsilon$	0	$-\varepsilon$	0	∞	∞	∞
2	0	∞	∞	∞	$-\varepsilon$	0	$-\varepsilon$	∞	∞	∞	∞	0	$-\varepsilon$	0
3	∞	∞	0	∞	∞	0	∞	∞	0	∞	0	0	∞	0
4	0	∞	∞	∞	$-\varepsilon$	0	$-\varepsilon$	∞	∞	∞	∞	0	$-\varepsilon$	0
5	0	0	∞	$-\varepsilon$	$-\varepsilon$	∞	$-\varepsilon$	$-\varepsilon$	∞	$-\varepsilon$	∞	∞	$-\varepsilon$	∞
6	∞	0	0	$-\varepsilon$	∞	∞	∞	$-\varepsilon$	0	$-\varepsilon$	0	∞	∞	∞

a linked (not linked) state with respect to the former. Such condition can be imposed by assigning infinite energy penalties to nearest neighbor pair states that violate the connectivity constraint (infinite energies can be treated numerically as vanishing Boltzmann weights). The self-avoiding condition is guaranteed by the set of site configurations (Table I), which does not include self-crossing. One more constraint to be satisfied is the absence of closed loops on every d cube of the Husimi tree, otherwise the model would describe a mixture of infinite length polymers and of small closed-loop molecules, with different thermodynamic properties. Also the last condition can be imposed by suitable infinite energy penalties.

Let us now show, how we can investigate the SAW gas on the class of cactus trees defined above. We shall take the square cactus as an example, then we shall see that a formally equivalent method can be employed for any dimension. The Hamiltonian $\mathcal{H}$ of the system (which includes interaction energies, bending energies, chemical potential contributions, and also the fictitious energies needed to impose the constraints) can be written as a sum over the squares in the following way:

$$\mathcal{H}=\sum_m H(\{\sigma_{\mathbf{k}}^{(m)}\}), \tag{1}$$

where $H(\{\sigma_{\mathbf{k}}^{(m)}\})$ is the contribution of the mth square (square Hamiltonian), and

$$\{\sigma_{\mathbf{k}}^{(m)}\}\equiv\{\sigma_{00}^{(m)},\sigma_{01}^{(m)},\sigma_{10}^{(m)},\sigma_{11}^{(m)}\} \tag{2}$$

denotes the set of state variables in the square. Notice that state variables have a double label: m indicates that a variable refers to a site in the mth square, while $\mathbf{k}\equiv k_x k_y = 00,01,10,11$ denotes a particular site in the given square. Assuming that square sides have unit length and the lower left vertex is placed at the origin of a reference frame, k_x and k_y are vertex coordinates. The square Hamiltonian can be written as

$$H(\{\sigma_{k_xk_y}\})=\frac{1}{2}\sum_{k_xk_y=00}^{11}h(\sigma_{k_xk_y})+\sum_{k_y=0}^{1}u_x(\sigma_{0k_y},\sigma_{1k_y})+\sum_{k_x=0}^{1}u_y(\sigma_{k_x0},\sigma_{k_x1})+v(\sigma_{00},\sigma_{01},\sigma_{10},\sigma_{11}). \tag{3}$$

In the last equation h denotes site energy terms, which take into account bending energies and chemical potential contributions. They are defined as

$$h(\sigma)=\chi n_{\mathrm{b}}(\sigma)-\mu n_{\mathrm{o}}(\sigma), \tag{4}$$

where $n_{\mathrm{o}}(\sigma)$ are "occupation" numbers, defined as $n_{\mathrm{o}}(\sigma)=0$ for $\sigma=0$ (empty site), $n_{\mathrm{o}}(\sigma)=1$ otherwise (occupied site), while $n_{\mathrm{b}}(\sigma)$ are "bending" numbers, defined as $n_{\mathrm{b}}(\sigma)=0$ for $\sigma\leqslant 2$ (straight segment or empty site), $n_{\mathrm{b}}(\sigma)=1$ otherwise (bent segment). Normalization to the connectivity constant 2 avoids multiple counting. Moreover, u_x and u_y represent pair interaction energies along the x and y axes, respectively (see Table II). They take into account also connectivity constraints, as previously mentioned. Let us notice that the difference between u_x and u_y does not correspond to a real anisotropic interaction, but is due to the fact that site states are defined with respect to a fixed reference frame. Finally, the four site term v takes into account that square loops are forbidden. It is defined as $v(3,6,4,5)=\infty$, $v(\sigma_{00},\sigma_{01},\sigma_{10},\sigma_{11})=0$ otherwise.

The thermodynamics of a cactus system can be investigated exactly, in a numerical way, taking into account self-similarity, that is, by solving a suitable recursion relation [20]. First one has to define partial partition functions (PPFs). Let us consider a branch of our cactus tree, for instance the one depicted in Fig. 1(c), and a corresponding partial Hamiltonian, obtained by Eq. (1) with the sum restricted to squares in the branch. The corresponding PPF $W(\sigma)$ can be computed by summing Boltzmann weights of the partial Hamiltonian over the states of the branch minus the base site, which is characterized by the σ state variable. Of course, the PPF tends to infinity in the thermodynamic limit, that is, for an infinite generation branch, so it is convenient to define a normalized PPF $w(\sigma)\propto W(\sigma)$ in such a way that

TABLE III. Definition of reflection operators $\mathcal{R}_{\mathbf{k}}:\sigma\mapsto\mathcal{R}_{\mathbf{k}}\sigma$, in $d=2$. Notice that $\mathcal{R}_{11}=\mathcal{R}_{10}\mathcal{R}_{01}$ (see the text).

σ	0	1	2	3	4	5	6
$\mathcal{R}_{10}\sigma$	0	1	2	4	3	6	5
$\mathcal{R}_{01}\sigma$	0	1	2	6	5	4	3

$$\sum_{\sigma} w(\sigma)=1. \tag{5}$$

From symmetry arguments it is easy to see that, if the base site of the branch is $\mathbf{k}$ instead of $\mathbf{0}\equiv 00$, the corresponding PPF can be written as

$$w_{\mathbf{k}}(\sigma)=w(\mathcal{R}_{\mathbf{k}}\sigma), \tag{6}$$

where $\mathcal{R}_{\mathbf{k}}$ is a ''reflection'' operator, which, acting on a site configuration σ, returns the $\mathcal{R}_{\mathbf{k}}\sigma$ configuration, obtained by a reflection of σ with respect to the plane orthogonal to the $\mathbf{k}$ vector. In Table III, we report explicit definitions of the reflection operators. Let us notice that the following composition rule holds:

$$\mathcal{R}_{\mathbf{k}}\mathcal{R}_{\mathbf{k}'}=\mathcal{R}_{\mathbf{k}\oplus\mathbf{k}'}, \tag{7}$$

where $\oplus$ denotes the ''bit-per-bit'' logical exclusive or (defined by $0\oplus 0=1\oplus 1=0$, $0\oplus 1=1\oplus 0=1$). Let us now consider again the branch depicted in Fig. 1. In the infinite generation limit, and in the hypothesis of a homogeneous system, the subbranches attached to the first square of the branch should be equivalent to main one. So the corresponding PPFs do not depend on the m (square) label, and one can write the recursion relation

$$w(\sigma_{\mathbf{0}})=g^{-1}\sum_{\{\sigma_{\mathbf{k}}\}_{\mathbf{k}\neq\mathbf{0}}} e^{-\beta H(\{\sigma_{\mathbf{k}}\})}\prod_{\mathbf{k}\neq\mathbf{0}} w_{\overline{\mathbf{k}}}(\sigma_{\mathbf{k}}), \tag{8}$$

where the sum runs over state variables in the square except $\sigma_{\mathbf{0}}$, $\beta=1/KT$ (K being the Boltzmann constant and T the absolute temperature), a bar denotes the bit-per-bit logical inversion (defined by $\overline{0}=1$, $\overline{1}=0$), and g is a normalization constant, imposed by Eq. (5). The recursion relation can be iterated numerically to determine a fixed point, which represents the PPF of a branch whose base site lies in the bulk of the cactus tree. Bulk properties of the cactus system are assumed to approximate the ordinary lattice system. For each site $\mathbf{k}$ in a square, we can compute the probability distribution $p_{\mathbf{k}}(\sigma)$ of the corresponding state variable, by considering the operation of attaching two branches to the given site. We obtain

$$p_{\mathbf{k}}(\sigma)=z^{-1}w_{\mathbf{k}}(\sigma)w_{\overline{\mathbf{k}}}(\sigma), \tag{9}$$

where of course $w_{\mathbf{0}}(\sigma)\equiv w(\sigma)$, while

$$z=\sum_{\sigma} w_{\mathbf{k}}(\sigma)w_{\overline{\mathbf{k}}}(\sigma) \tag{10}$$

provides normalization. Let us notice that z turns out to be independent of $\mathbf{k}$, due to Eq. (6). The residual $\mathbf{k}$ dependence of the site probability distributions does not break homogeneity, because, according to Eq. (6), the following symmetry relationship holds:

$$p_{\mathbf{k}}(\sigma)=p_{\mathbf{0}}(\mathcal{R}_{\mathbf{k}}\sigma). \tag{11}$$

Therefore, the probability ρ that a site is visited by a walk, which we shall briefly refer to as *density* in the following, can be evaluated as:

$$\rho=1-p_{\mathbf{k}}(0), \tag{12}$$

independently of $\mathbf{k}$. The density ρ is the main order parameter for our system.

We have described the recursive approach for a square cactus, that is, for the $d=2$ case. Nevertheless, for $d=3$, we can develop a formally equivalent procedure, with the same equations, provided $\mathbf{k}$ denote cube vertices, that is, $\mathbf{k}=000,001,\ldots,111$, and the square Hamiltonian definition (3) is replaced by a suitable definition of cube Hamiltonian. Let us notice that in $d=3$ a computer program which performs a single iteration of the recursion relation (8) should consider in principle $16^8=4\,294\,967\,296$ cube configurations (16 being the number of possible site configurations, and 8 the number of vertices in a cube), making the calculation unfeasible. This huge number can be reduced to 3 746 978, if from the beginning one takes into account only configurations respecting connectivity. A suitable algorithm has been programmed to this purpose.

The starting values of the recursion relation represent boundary conditions on the surface of the cactus trees. Moreover, the fixed point represents the bulk equilibrium state, and phase transitions can be detected in principle as changes of the fixed point, driven by model parameters. In this way, one determines the actual phase behavior of a cactus system. Nevertheless, it is widely believed that in the presence of multiple fixed points (which can be reached from different boundary conditions), that is, in the presence of coexistence phenomena, the first-order transition which best approximates that of the ordinary lattice system can be obtained by minimizing the bulk free energy density [19,20]. For our system, the suitable free energy density is the excess grand potential per site ω referred to pure solvent. Such a potential can be evaluated as

$$\omega=-KT\left[\frac{1}{2^{d-1}}\ln g-\left(1-\frac{1}{2^{d-1}}\right)\ln z\right], \tag{13}$$

where g is the normalization constant of the recursion relation (8) and z is given by Eq. (10). The derivation requires some manipulations and is left to the Appendix. From the knowledge of the grand potential one can derive all other thermodynamic properties.

III. THE PHASE DIAGRAMS AND THE DILUTE SOLUTION LIMIT

In the framework of a grand-canonical description, the phase diagram can be determined as a function of temperature and chemical potential. For a SAW the latter controls the

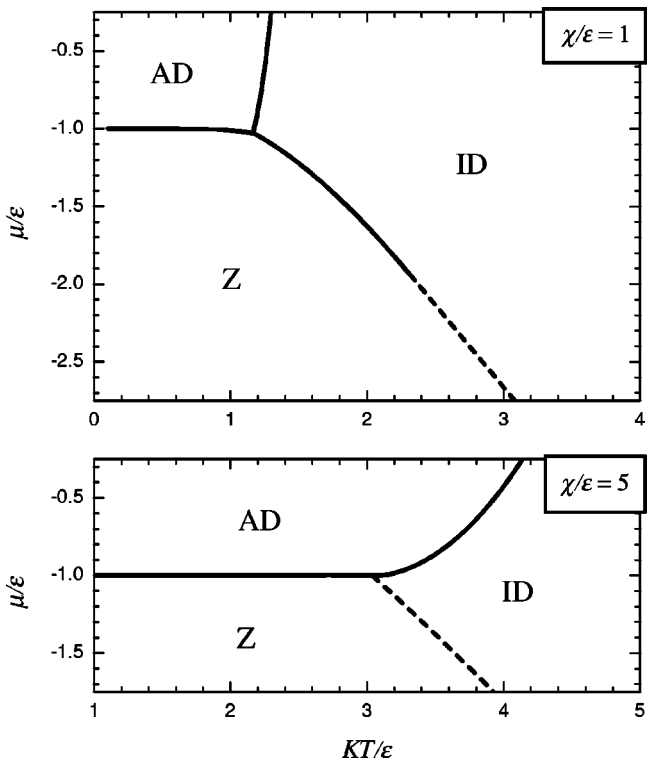

FIG. 2. Chemical potential-temperature (μ/ε vs KT/ε) phase diagram in $d=2$ for a low stiffness case ($\chi/\varepsilon=1$, upper graph) and a high stiffness case ($\chi/\varepsilon=5$, lower graph). Solid lines denote first-order transitions; dashed lines denote second-order transitions. The zero density phase ($\rho=0$) is denoted by *Z*, the isotropic dense phase ($0<\rho<1$) by ID, and the anisotropic saturated phase ($\rho=1$) by AD.

average chain length. For example, in the simple Θ model [5] there exists a phase transition line $\mu=\mu^*(T)$ at which (for increasing μ values) the average length either diverges continuously (for temperatures higher than some temperature T_Θ) or jumps discontinuously to infinity (for temperatures lower than T_Θ). The transition line is identified as the thermodynamic limit of an isolated chain in solution. The system can be also described in terms of the density ρ, and one obtains $\rho=0$ for $\mu<\mu^*(T)$ and $\rho>0$ for $\mu>\mu^*(T)$. From the dense region of the phase diagram the transition line can be seen as the dilute solution limit (a single chain in solution). The transition is second order for $T>T_\Theta$ and first order for $T<T_\Theta$. The tricritical point $[T_\Theta,\mu^*(T_\Theta)]$, known as Θ point, represents the coil-globule collapse. Let us notice that, in our description, walks cannot terminate except on the lattice boundaries (see Table I), hence in the thermodynamic limit polymers are infinite in length even in the zero density phase. This is not expected to affect the phase behavior of an equilibrium system. We now present grand-canonical phase diagrams of the 2D semiflexible model in the cactus approximation for a low stiffness case ($\chi/\varepsilon=1$) and a high stiffness case ($\chi/\varepsilon=5$), which show qualitatively different behaviors.

Let us consider the low stiffness case first. The phase diagram is displayed in Fig. 2 (upper graph), where the temperature variable is KT/ε and the chemical potential variable is μ/ε. We find three different phases: the zero density (*Z*) phase, the isotropic dense (ID) phase, and the anisotropic dense (AD) phase. The *Z* phase is characterized by $\rho=0$ and $\omega=0$. Let us notice that the excess grand potential was expected to vanish in the *Z* phase, in which only a vanishing fraction of sites is visited by a walk. In the remainder of the article, we shall understand that all thermodynamic quantities are excess quantities referred to pure solvent. The ID phase is characterized by $0<\rho<1$, and corresponds to the dense phase of the ordinary Θ model. In the cactus approximation, we say that the ID phase is ''isotropic,'' meaning that the probability of having a straight segment is independent of the direction, that is $p_{\mathbf{k}}(1)=p_{\mathbf{k}}(2)$. Otherwise, the system does not possess a real invariance under 90° rotation, due to the cactus structure itself. The AD phase is anisotropic, in the sense that $p_{\mathbf{k}}(1)\neq p_{\mathbf{k}}(2)$, and saturated ($\rho=1$), that is, it describes a Hamiltonian walk. Most sites are occupied by chain segments aligned to a coordinate axis. The transition line between the *Z* and ID phases turns out to be partially first and partially second order. The two regimes are separated by a tricritical point, which is an ordinary Θ point. In the dense region ($\rho>0$) a first-order transition line separates the ID and AD phases. As far as the high stiffness case is concerned, the phase diagram is reported in the lower graph of Fig. 2. The same three phases *Z*, ID, and AD discussed above are present, even if the topology of the phase diagram is different. The *Z*-ID transition line is totally second order, so the tricritical point disappears, and is replaced by a critical end point. This corresponds to a discontinuous collapse, instead of the ordinary (continuous) Θ collapse.

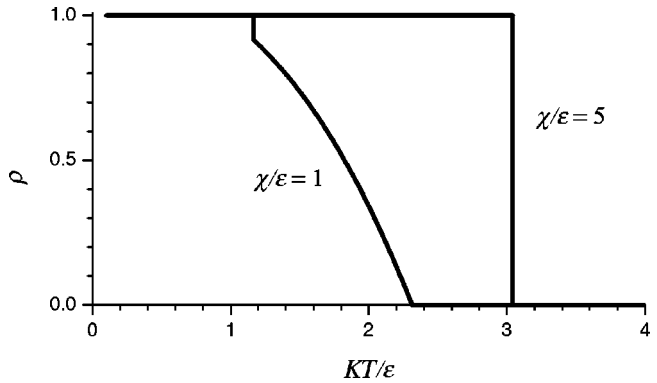

FIG. 3. Density as a function of temperature (ρ vs KT/ε) in the dilute solution limit in $d=2$ for the low ($\chi/\varepsilon=1$) and high ($\chi/\varepsilon=5$) stiffness cases.

As previously mentioned, we are mainly interested in the dilute solution limit, that is, in the transition between the *Z* phase and the dense phases, because it describes a single chain in solution. So we shall give more detailed results about this issue. The density ρ, computed in the limit of μ tending to the transition line from above, which denotes the chain compactness, is reported in Fig. 3 as a function of temperature. In the high stiffness ($\chi/\varepsilon=5$) case, one finds a single abrupt transition from $\rho=1$ to $\rho=0$, upon increasing temperature. In the lower temperature region the polymer is in the anisotropic (*A*) compact state, while in the higher temperature one the polymer is in the swollen coil (*C*) state. The low stiffness case ($\chi/\varepsilon=1$) displays three different phases. The lowest temperature one is *A*, like in the high stiffness

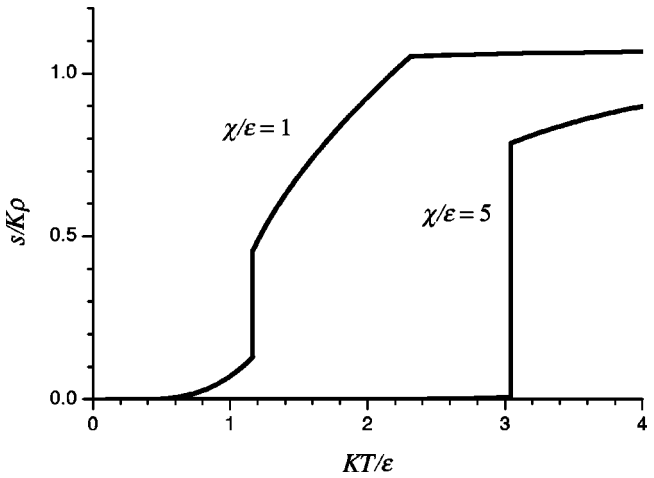

FIG. 4. Entropy per monomer as a function of temperature ($s/K\rho$ vs KT/ε) in the dilute solution limit in $d=2$ for the low ($\chi/\varepsilon=1$) and high ($\chi/\varepsilon=5$) stiffness cases.

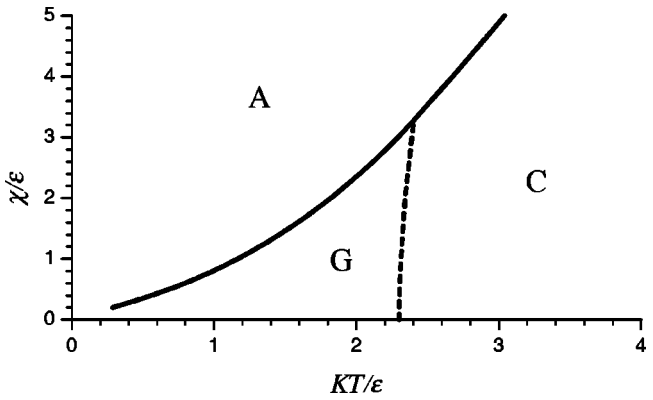

FIG. 5. Stiffness-temperature (χ/ε vs KT/ε) phase diagram in the dilute solution limit in $d=2$. Solid lines denote first-order transitions; a dashed line denotes the Θ transition. The coil phase is denoted by *C*, the isotropic globule phase by *G*, and the anisotropic phase by *A*.

case. At some temperature the system undergoes a first-order transition, in which the chain becomes orientationally disordered, but its density does not fall down to zero. This phase may be identified with the ordinary compact globule (*G*) observed in the Θ model. Upon further increasing temperature, the density decreases continuously, reaching zero at an ordinary Θ point, after which the polymer is again in a *C* state.

We also investigate the temperature dependence of the entropy per monomer in the dilute solution limit. It can be computed in the following way. The grand potential per site can be written as

$$\omega = f - \mu\rho, \tag{14}$$

where f is the Helmholtz free energy per site. As previously mentioned, ω vanishes on the *Z* phase boundary, hence in this case, μ coincides with the Helmholtz free energy per monomer,

$$\mu = f/\rho, \tag{15}$$

for a single chain in solution. Assuming that

$$\mu/\varepsilon = \varphi(KT/\varepsilon) \tag{16}$$

defines the *Z* phase boundary (which is known numerically, see Fig. 2), we can derive the entropy per monomer as

$$s/\rho = -K\varphi'(KT/\varepsilon), \tag{17}$$

where φ' denotes the first derivative of φ. The entropy, normalized to *K*, is displayed in Fig. 4 as a function of temperature. Let us notice that in the *A* state the entropy is low, but not zero. In the low stiffness case it jumps to a higher value in the *G* state, reflecting orientational disordering, then it increases on increasing temperature. The slope becomes abruptly lower at the Θ point. On the contrary, in the high stiffness regime, there is a direct jump to the high entropy value associated to the highly disordered *C* state.

All the qualitative features, we have described for the two regimes observed in $d=2$ are preserved in $d=3$, so we do not report the corresponding graphs. Rather let us notice that the dilute solution behavior is in qualitative agreement with Monte Carlo simulations of a single semiflexible chain on a 3D (simple cubic) lattice [9,10]. This supports the reliability of the cactus approximation in the analysis of lattice polymer models. On the contrary, the classical mean-field approach was not able to describe the first-order collapse in the high stiffness regime [8]. The Bethe approximation, equivalent to the cactus approximation for a Cayley tree, does describe the two regimes, but has been shown to introduce some artifacts [13]. For example, the anisotropic phase turns out to be completely frozen, that is, all lattice sites are occupied by straight segments aligned to a coordinate axis, and the entropy is rigorously zero even at finite temperature. As shown above, the cactus approximation predicts a nonvanishing entropy, which suggests that it is capable of describing some degree of (local) disorder even for the saturated phase.

In order to perform a more detailed comparison with Monte Carlo simulations [9,10], we now systematically characterize the dilute solution behavior, by investigating a continuous range of values of the stiffness parameter. Let us start again from $d=2$. Figure 5 shows the phase diagram as a function of stiffness and temperature. The two regimes can be easily recovered, and, quantitatively, we find the boundary of the low stiffness regime at $\chi/\varepsilon \approx 3.29$. Let us notice that, for very low stiffness values, the *A*-*G* transition line seems to disappear. Actually in this region the convergence of the recursion relation is very slow, which suggests the presence of a tricritical point and of a subsequent critical transition. This is shown more clearly by the corresponding stiffness-entropy phase diagram (Fig. 6), where the entropies of the *A* and *G* phases tend to coincide, as *A* becomes less and less anisotropic, and structurally similar to *G*. Such behavior is a peculiarity of the $d=2$ case. For $d=3$ the stiffness-temperature phase diagram is reported in Fig. 7, together with the results of Monte Carlo simulations [9,10]. The qualitative agreement is good, even if, from a quantitative point of view, the cactus approximation overestimates (as all mean-field-like approximations) the stability of the more ordered phase. Nevertheless, it is remarkable that the cactus

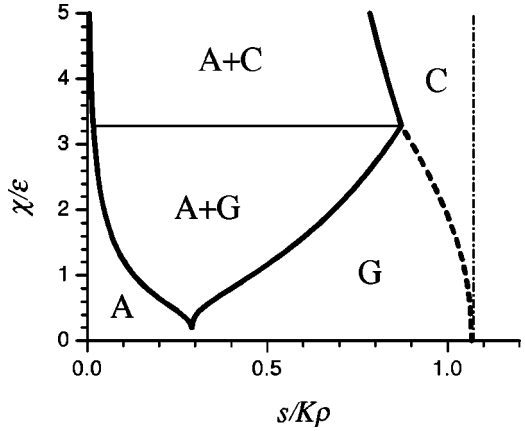

FIG. 6. Stiffness entropy per monomer (χ/ε vs $s/K\rho$) phase diagram in the dilute solution limit in $d=2$. Thick solid lines denote boundaries of pure phase regions; a dashed line denotes the Θ transition. A thin solid line denotes the critical end point; a dash-dotted line denotes the athermal limit $T\to\infty$. Tags are as in Fig. 5. Double tags denote coexistence regions.

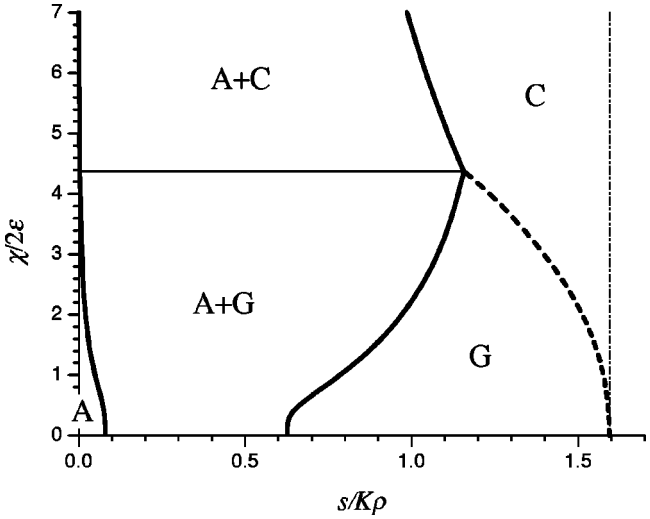

FIG. 8. Stiffness entropy per monomer ($\chi/2\varepsilon$ vs $s/K\rho$) phase diagram in the dilute solution limit in $d=3$. Lines and tags are as in Fig. 6.

approximation is also able to reproduce, though not quantitatively, the increasing trend of the C-G transition (Θ) temperature as a function of stiffness. As far as this issue is concerned, let us remind that both the classical mean-field approach and the Bethe approximation predict a rigorously stiffness independent Θ temperature. Finally, Fig. 8 shows the stiffness-entropy phase diagram for $d=3$. It turns out to be qualitatively different from the corresponding $d=2$ diagram, in that the A-G transition clearly does not tend to criticality even for vanishing stiffness, as the corresponding entropies are significantly different. Such a detail seems to suggest that the cactus approximation is also capable of discriminating dimension dependent effects.

IV. CONCLUSIONS

We have investigated a cactus approximation for a lattice polymer model with attractive short range interaction and stiffness. The semiflexible model has been already investigated by means of different techniques, and has been suggested to have some relevance also in the description of some biopolymer properties. In this paper, we have considered the performance of the cactus approximation in the analysis of such model. The method turns out to require a reasonable computational effort also in 3D, yielding qualitatively correct results, compared to more accurate techniques. Moreover, it allows one to study phase diagrams and thermodynamic properties in full detail, due to relatively small numerical complexity.

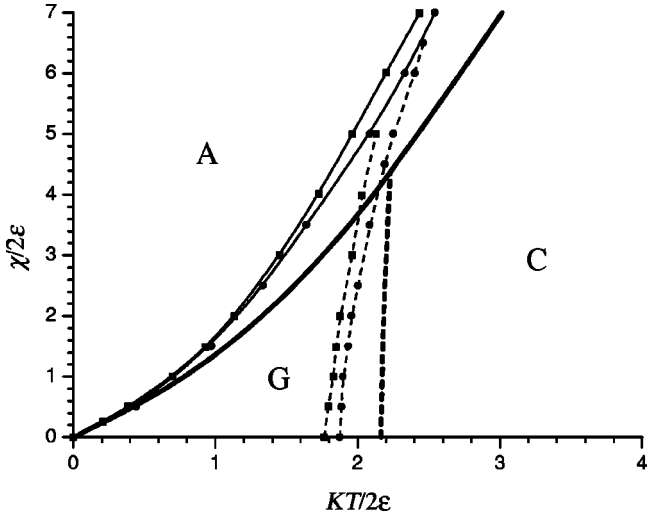

FIG. 7. Stiffness-temperature ($\chi/2\varepsilon$ vs $KT/2\varepsilon$) phase diagram in the dilute solution limit in $d=3$. Circles and squares denote results of the Monte Carlo simulations of Refs. [9,10], respectively. Thin lines are eye guides. Other lines and tags are as in Fig. 5.

The model shows two qualitatively different behaviors, depending on stiffness. For high stiffness values, a polymer in dilute solution undergoes a first-order collapse from a swollen coil at high temperature to an extremely compact anisotropic state at low temperature. Lower stiffness values yield a qualitatively different behavior. Upon increasing temperature the polymer chain undergoes two phase transitions: from the anisotropic state to an isotropic globule, and then from globule to coil (Θ transition). The cactus approximation qualitatively reproduces the two different behaviors. For both cases, we have computed the most relevant thermodynamic functions, namely, the Helmholtz free energy and entropy per monomer as a function of temperature.

We have compared our results for the dilute solution limit with those of Monte Carlo simulations, and of other mean-field like approximations. The classical mean-field approach does not succeed in describing the first-order collapse at high stiffness values. The Bethe approximation does describe two regimes, but introduces artifacts. First of all, the anisotropic phase turns out to be completely frozen even at finite temperature, with all chain segments aligned to a privileged direction, and zero configurational entropy. On the contrary, the cactus approximation predicts a nonvanishing entropy, that is, some degree of configurational disorder. Moreover, both the mean-field theory and the Bethe approximation predict a rigorously stiffness independent Θ collapse temperature, while, remarkably, the cactus approximation qualitavely

reproduces the increasing trend of the transition temperature, upon increasing the stiffness parameter. Finally, the 2D cactus approximation displays a peculiarity in the anisotropic-isotropic transition, which tends to criticality for ti very low stiffness. Therefore, the cactus approximation turns out to be sensitive to dimensionality, while the Bethe approximation seems to be quite insensitive, predicting an all first-order transition line also in two dimensions.

On the basis of these results, we suggest that the cactus approximation may be a reliable tool to get qualitative information about the thermodynamics of lattice polymer models.

APPENDIX: BULK FREE ENERGY DENSITY

In this appendix, we explain the formula employed in the text to evaluate the bulk free energy density. It is known that the contribution F of each (bulk) d cube to the total free energy can be written exactly as [20]

$$\beta F = \left\langle \beta H(\{\sigma_{\mathbf{k}}\}) + \ln P(\{\sigma_{\mathbf{k}}\}) - \frac{1}{2}\sum_{\mathbf{k}} \ln p_{\mathbf{k}}(\sigma_{\mathbf{k}}) \right\rangle, \tag{A1}$$

where $\langle \cdot \rangle$ denotes an ensemble average over the d-cube state variables, and $P(\{\sigma_{\mathbf{k}}\})$ is the joint probability distribution of such variables. Let us notice that here F denotes a generic free energy, not necessarily the Helmholtz one. It is easy to see that

$$P(\{\sigma_{\mathbf{k}}\}) = Z^{-1} e^{-\beta H(\{\sigma_{\mathbf{k}}\})} \prod_{\mathbf{k}} w_{\overline{\mathbf{k}}}(\sigma_{\mathbf{k}}), \tag{A2}$$

where

$$Z = \sum_{\{\sigma_{\mathbf{k}}\}} e^{-\beta H(\{\sigma_{\mathbf{k}}\})} \prod_{\mathbf{k}} w_{\overline{\mathbf{k}}}(\sigma_{\mathbf{k}}) \tag{A3}$$

provides normalization. Replacing Eq. (A2) and Eq. (9) into Eq. (A1), and taking into account the linearity of the average operation, one obtains

$$\beta F = -\ln Z + \frac{1}{2}\sum_{\mathbf{k}} \ln z + \frac{1}{2}\Phi, \tag{A4}$$

where

$$\Phi = \sum_{\mathbf{k}} \left\langle \ln \frac{w_{\overline{\mathbf{k}}}(\sigma_{\mathbf{k}})}{w_{\mathbf{k}}(\sigma_{\mathbf{k}})} \right\rangle. \tag{A5}$$

By expanding the statistical average, the last term reads

$$\Phi = \sum_{\mathbf{k}} \sum_{\sigma} p_{\mathbf{k}}(\sigma)[\ln w_{\overline{\mathbf{k}}}(\sigma) - \ln w_{\mathbf{k}}(\sigma)]. \tag{A6}$$

Due to the fact that the sum is taken over all $\mathbf{k}$, one can also write

$$\Phi = \sum_{\mathbf{k}} \sum_{\sigma} [p_{\overline{\mathbf{k}}}(\sigma) - p_{\mathbf{k}}(\sigma)] \ln w_{\mathbf{k}}(\sigma). \tag{A7}$$

From Eq. (9), it is easy to see that

$$p_{\overline{\mathbf{k}}}(\sigma) = p_{\mathbf{k}}(\sigma), \tag{A8}$$

whence $\Phi = 0$. As a consequence, Eq. (A4) in d dimensions reads

$$\beta F = -\ln Z + 2^{d-1} \ln z. \tag{A9}$$

Let us notice that Z involves a sum over all d-cube state variables, hence it is quite expensive to be computed numerically for $d = 3$. Nevertheless, making use of Eqs. (A3), (8), and (10), it is possible to show that

$$Z = gz, \tag{A10}$$

where g is the normalization constant of the recursion relation (8), which has to be computed at each iteration. Moreover, as previously mentioned, F is actually the free energy density per d cube, related to the free energy density per site f by

$$F = 2^{d-1} f \tag{A11}$$

(each d cube contains 2^d sites, but each site is shared by 2 d cubes). Thus, one can finally write

$$\beta f = -\frac{1}{2^{d-1}} \ln g + \left(1 - \frac{1}{2^{d-1}}\right) \ln z. \tag{A12}$$

[1] J. des Cloizeaux and G. Jannink, *Polymers in Solution: Their Modelling and Structure* (Clarendon Press, Oxford, 1990).

[2] C. Vanderzande, *Lattice Models of Polymers* (Cambridge University Press, Cambridge, 1998).

[3] P.J. Flory, *Principles of Polymer Chemistry* (Cornell University Press, Ithaca, NY, 1971).

[4] P.G. de Gennes, *Scaling Concepts in Polymer Physics* (Cornell University Press, Ithaca, NY, 1988).

[5] P.G. de Gennes, Phys. Lett. A **38**, 339 (1972).

[6] J. Bascle, T. Garel, and H. Orland, J. Phys. II **3**, 245 (1993).

[7] T.E. Creighton, *Proteins: Structures and Molecular Properties* (Freeman, New York, 1996).

[8] S. Doniach, T. Garel, and H. Orland, J. Chem. Phys. **105**, 1601 (1996).

[9] U. Bastolla and P. Grassberger, J. Stat. Phys. **89**, 1061 (1997).

[10] J.P.K. Doye, R.P. Sear, and D. Frenkel, J. Chem. Phys. **108**, 2134 (1998).

[11] J.F. Stilck, K.D. Machado, and P. Serra, Phys. Rev. Lett. **76**,

2734 (1996); *ibid.* **89**, 169602 (2002).
[12] M. Pretti, Phys. Rev. Lett. **89**, 169601 (2002).
[13] S. Lise, A. Maritan, and A. Pelizzola, Phys. Rev. E **58**, R5241 (1998).
[14] P. Bruscolini, C. Buzano, A. Pelizzola, and M. Pretti, Phys. Rev. E **64**, 050801(R) (2001).
[15] H.A. Bethe, Proc. R. Soc. London, Ser. A **150**, 552 (1935).
[16] E.A. Guggenheim, *Mixtures* (Oxford University, London, 1952).
[17] R. Kikuchi, Phys. Rev. **81**, 988 (1951).
[18] R. Kikuchi, J. Chem. Phys. **60**, 1071 (1974).
[19] P.D. Gujrati, Phys. Rev. Lett. **74**, 809 (1995).
[20] M. Pretti, J. Stat. Phys. (to be published).